

**MATERIALS
CHEMISTRY**
FRONTIERS



The selective blocking of potentially catalytically-active sites on surface-supported iron oxide catalysts

Journal:	<i>Materials Chemistry Frontiers</i>
Manuscript ID	QM-RES-10-2022-001025.R2
Article Type:	Research Article
Date Submitted by the Author:	22-Dec-2022
Complete List of Authors:	Liu, Dairong; University of Illinois Chicago, Chemistry Li, Linfei; UIC, A. Gedara, Buddhika; University of Illinois Chicago, Chemistry Trenary, Michael; University of Illinois at Chicago, Chemistry Jiang, Nan; University of Illinois Chicago, Chemistry

SCHOLARONE™
Manuscripts

The selective blocking of potentially catalytically-active sites on surface-supported iron oxide catalysts

Dairong Liu,^a Linfei Li,^a Buddhika S. A. Gedara,^a Michael Trenary,^a Nan Jiang^{*a}

^aDepartment of Chemistry, University of Illinois Chicago, Chicago, Illinois 60607, USA

*Corresponding Author

Email: njiang@uic.edu

Abstract

The extensive research on ultrathin ferrous oxide (FeO) islands and films over the last few decades has significantly contributed to the understanding of their structural and catalytic properties. In this regard, the local chemical properties of FeO edges, such as their metal affinity, play a critical role in determining and tuning the catalytic reactivity of FeO, which however remains largely unexplored. In this work, we use scanning tunneling microscopy (STM) to study the interaction of Pd and Pt with FeO grown on Au(111). Different Fe affinities for Pd and Pt are demonstrated by the preferential growth of Pd on the Fe-terminated edge and Pt on the O-terminated edge of FeO nanoislands, resulting in selectively blocked FeO edges. In addition to revealing the different metal affinities of FeO edges, our results provide new insights into the edge reactivity of FeO/Au(111) and suggest an approach for controlling the selectivity of FeO catalysts.

Introduction

The utility of iron oxides in surface catalysis has been recognized since the 1970s and has resulted in extensive industrial applications like the Fischer-Tropsch reaction and the synthesis of styrene due to their unique chemical properties.¹⁻⁷ In view of its chemical instability, the synthesis and characterization of FeO benefit from ultrahigh vacuum (UHV) conditions, where ultrathin ferrous oxide (FeO) films are prepared by oxidizing iron on various metal surfaces, such as Pt(111)^{5, 8-11}, Pt (100)¹², Pd(111),¹³ Pd(100),¹⁴ Mo(100),¹⁵ Cu(001),¹⁶ Cu(110),¹⁷ Ru(0001),^{18, 19} Au(111),²⁰⁻²⁶ Ag(100),^{27, 28} and Ag(111).^{29, 30} The structure and properties of supported FeO are variable and heavily dependent on its interaction with the substrate. For example, in contrast to Pt(111), the inert Au(111) surface has proved to have a weak interaction with FeO, thereby allowing the intrinsic structural and chemical properties of FeO to be probed.^{22, 26, 31-35}

As a prototypical reaction in heterogeneous catalysis, carbon monoxide (CO) oxidation has been extensively studied to explore the catalytic properties of FeO.^{23, 36-42} During CO oxidation, the coordinately unsaturated ferrous sites (CUFs)⁴³, contribute significantly by activating O₂ adsorbed

therein and then oxidizing FeO edges into highly reactive FeO_x structures.^{22, 31, 43-45} Next, CO oxidation occurs by reducing the FeO_x at CUFs.⁴⁶ Therefore, FeO edges with CUFs play an essential role in initiating catalytic reactions of FeO. In-situ scanning tunneling microscopy (STM) studies highlighted the importance of FeO edges to CO oxidation, which facilitate the formation of oxidized and reduced FeO phases where CO oxidation occurs.^{33, 46} Early studies established a sole type of FeO edge, i.e., Fe-terminated edges with two-fold coordinated Fe atoms, which is associated with a triangular shape model of FeO. However, some FeO islands were later found to have a truncated triangular (or hexagonal) shape with preferred long edges and non-preferred short edges,^{39, 43} suggesting a second type of edge.^{47, 48} The second edge type was assigned to Fe-terminated edges with single-fold coordinated Fe atoms based on STM characterizations.⁴⁷ Further studies identified the second type of edge as O-terminated edges by X-ray photoelectron spectroscopy (XPS) and temperature-programmed desorption (TPD).^{48, 49} Consequently, FeO islands typically possess three Fe-terminated edges (Fe-edges) and three O-terminated edges (O-edges).⁵⁰ Moreover, Zeuthen et al. pointed out that under an oxygen-rich environment, O-edges are recognized as long and preferred edges, while under oxygen-poor conditions, the long edges are assigned as Fe-edges.¹³ Furthermore, because the synthesis of FeO requires annealing the sample to 600-700 K in UHV as the last step, the sample should be slightly reduced.^{24, 50} Therefore, the as-prepared FeO typically has three preferred longer Fe-edges and three non-preferred shorter O edges.⁵¹ In addition, three more types of FeO edges have been recently observed under mild oxidizing or reducing conditions,⁵¹ and in particular, edge-specific chemical properties were demonstrated in the oxidation and reduction of FeO.^{24, 50, 51} Although these studies underscore the distinct structural and chemical properties of FeO edges, well-controlled chemical modification of FeO edges remains to be explored despite its promise for modifying the chemistry and interfacial properties of FeO-based catalysts.

Herein, we establish an experimental strategy for chemically modifying FeO edges by selectively exposing Fe- or O-edges by blocking the other edges with transition metals (i.e., Pd and Pt). Specifically, UHV-STM imaging shows that deposited Pd atoms exclusively adsorb on the Fe-edges of FeO nano islands while Pt on the O-edges due to the different metal affinities of Fe-edges and O-edges.⁵² The resultant FeO islands expose only Fe- or O-edges, providing a platform for interrogating edge-specific chemical properties and gaining deeper insights into the catalytic performance of FeO nanostructures.

Methods

Synthesis of FeO/Au(111): All experiments were carried out in a UHV chamber ($\sim 2 \times 10^{-10}$ Torr). Clean Au(111) surfaces were prepared by repeated cycles of Ar⁺ sputtering and annealing to ~ 860 K and confirmed clean by STM. Fe was deposited onto Au(111) from an Fe rod (ESPI 99.999%) using a triple electron beam evaporator (EFM 3T, Omicron GmbH), the coverage of Fe is measured by STM images to be around 0.40 ML. The resulting Fe/Au(111) sample was then exposed to 1.2×10^{-5} Torr of O₂ for 15 min at room temperature. After annealing to ~ 760 K for 10 min and cooling down, the sample was transferred to the STM for characterization.

Preparation of Pd/Pt decorated FeO/Au(111): Pd or Pt was deposited onto as-prepared FeO/Au(111) by evaporating a Pd or Pt rod (ESPI 99.999%) from a EFM 3T evaporator. STM images indicate the coverage of Pd is around 0.05 ML while the Pt is around 0.04 ML. The sample was then annealed to 550 K to generate edge-blocked FeO/Au(111).

STM image acquisition and analysis: All STM studies were performed at room temperature with a variable temperature scanning probe microscope (VT-SPM, Omicron GmbH) using a chemically etched W tip under constant current mode. STM images were analyzed using the WSxM⁵³ program provided by Nanotech.

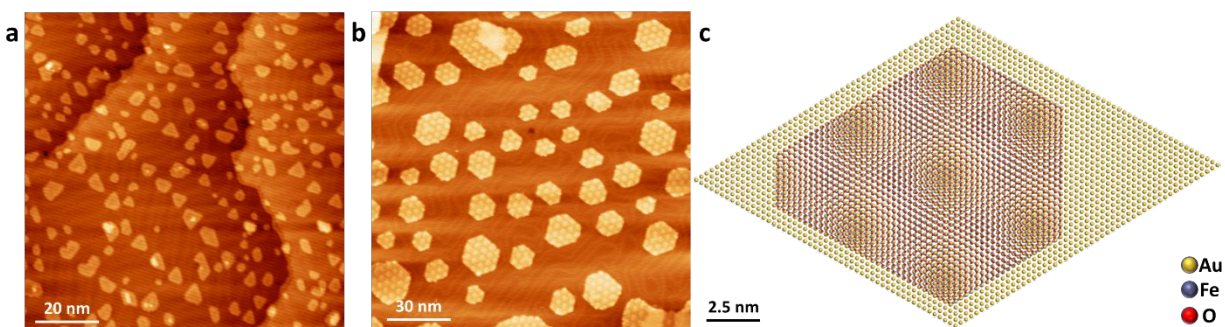


Fig. 1 Growth and structural properties of FeO on Au(111). (a) STM image of sub-monolayer Fe deposited on Au(111) ($V_{\text{bias}} = 1.2$ V, $I = 0.2$ nA). (b) STM topography of FeO islands ($V_{\text{bias}} = 1.5$ V, $I = 0.5$ nA). (c) Schematic illustration of the atomic structure of FeO/Au(111).

Results

The UHV synthesis of FeO began with the deposition of Fe single layers on Au(111),²¹ as shown in Fig. 1a. The sub-monolayer Fe was then exposed to O₂ at room temperature followed by annealing to ~760 K. The resulting FeO nanoislands are mostly in a truncated triangle shape with clear moiré superlattices (Fig. 1b), which stem from the lattice mismatch between FeO and Au(111) (Figs. 1c and 2c).²¹ As circled in Fig. 3, moiré patterns can be imaged as a triangular lattice (Fig. 3a) or honeycomb-like lattice (Fig. 3c), indicating a bias-dependent morphology.²⁵

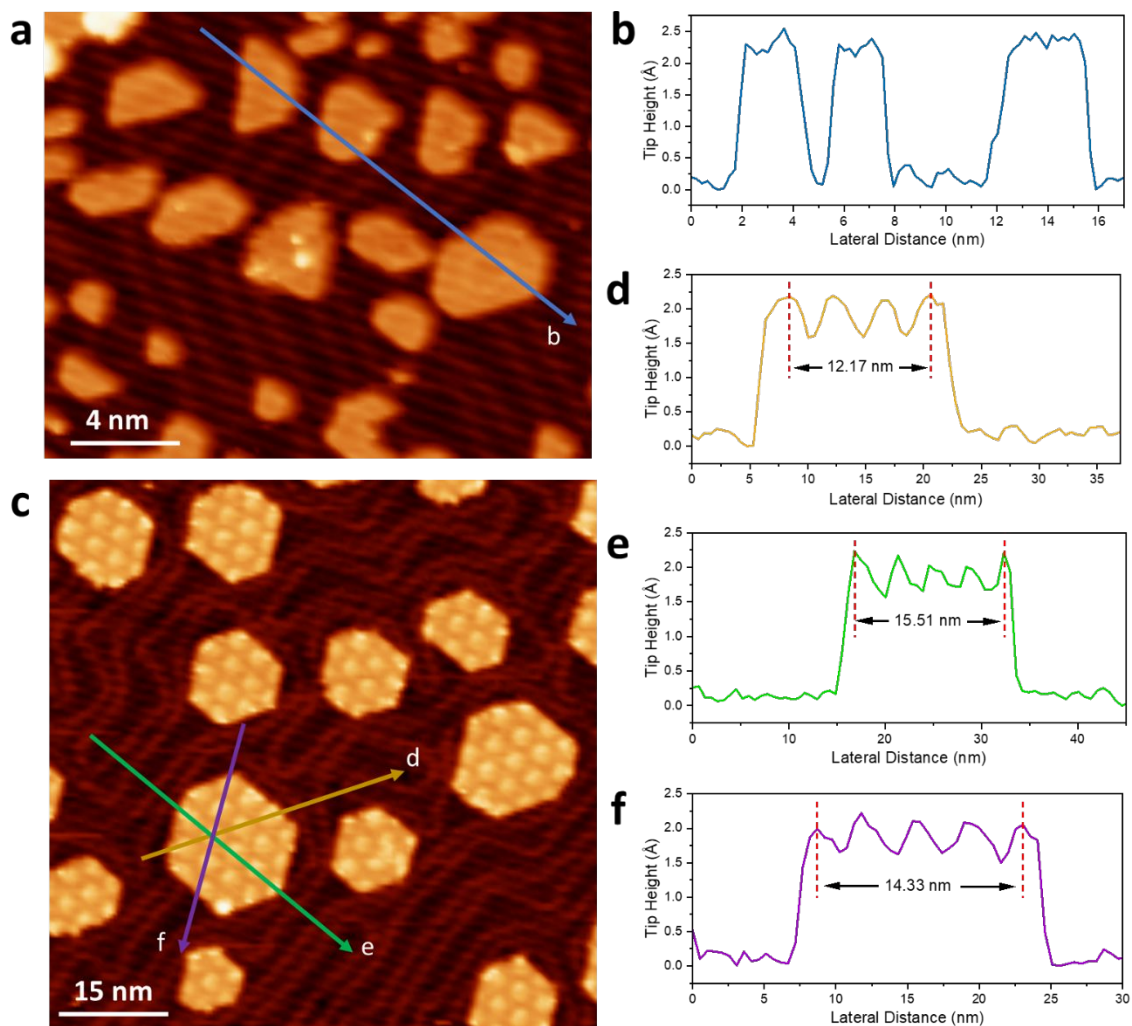


Fig. 2 (a) Fe islands deposited on Au(111) at room temperature ($V_{\text{bias}} = 1.2$ V, $I = 0.2$ nA); (b) Line profile of Fe/Au(111). Fe islands show a height of ~ 2.2 Å, which fits the height of single-layer Fe atoms; (c) FeO islands on the Au(111) surface ($V_{\text{bias}} = 1.5$ V, $I = 0.3$ nA); (d-f) Line profiles of FeO/Au(111). FeO islands show an average superlattice constant of ~ 3.84 nm, which is in the error range of the model shown in Fig. 1c when thermal drifting is considered.

An additional observation in Fig. 3a, c is the apparently dark FeO islands on Au(111) terraces and step edges (highlighted by white arrows), which show the same moiré patterns as those on the supported FeO islands (Fig. 3e-g) but -1 Å apparent height with respect to the Au(111) terrace. The 1 Å dip matches the height difference between a single Au(111) atomic step (~ 2.4 Å) and monolayer FeO (~ 1.5 Å), suggesting that the FeO islands are embedded into the surface plane of Au(111).^{21, 25, 26} Recent studies have demonstrated the growth mechanism of embedded FeO on Au(111), which involves the diffusion of Fe atoms into the Au subsurface after annealing, the resulting migration of the surrounding Au atoms, and the final formation of FeO islands with the addition of oxygen.^{54, 55} Notably, the CUFs of embedded FeO islands on Au terraces and step edges are all or partially buried, making the edges largely inaccessible to modification.^{43, 48} In contrast,

well-defined Fe- and O-edges are exposed on the supported FeO islands,²⁴ potentially allowing CUFs and thus catalytic properties to be modified in a well-controlled manner.

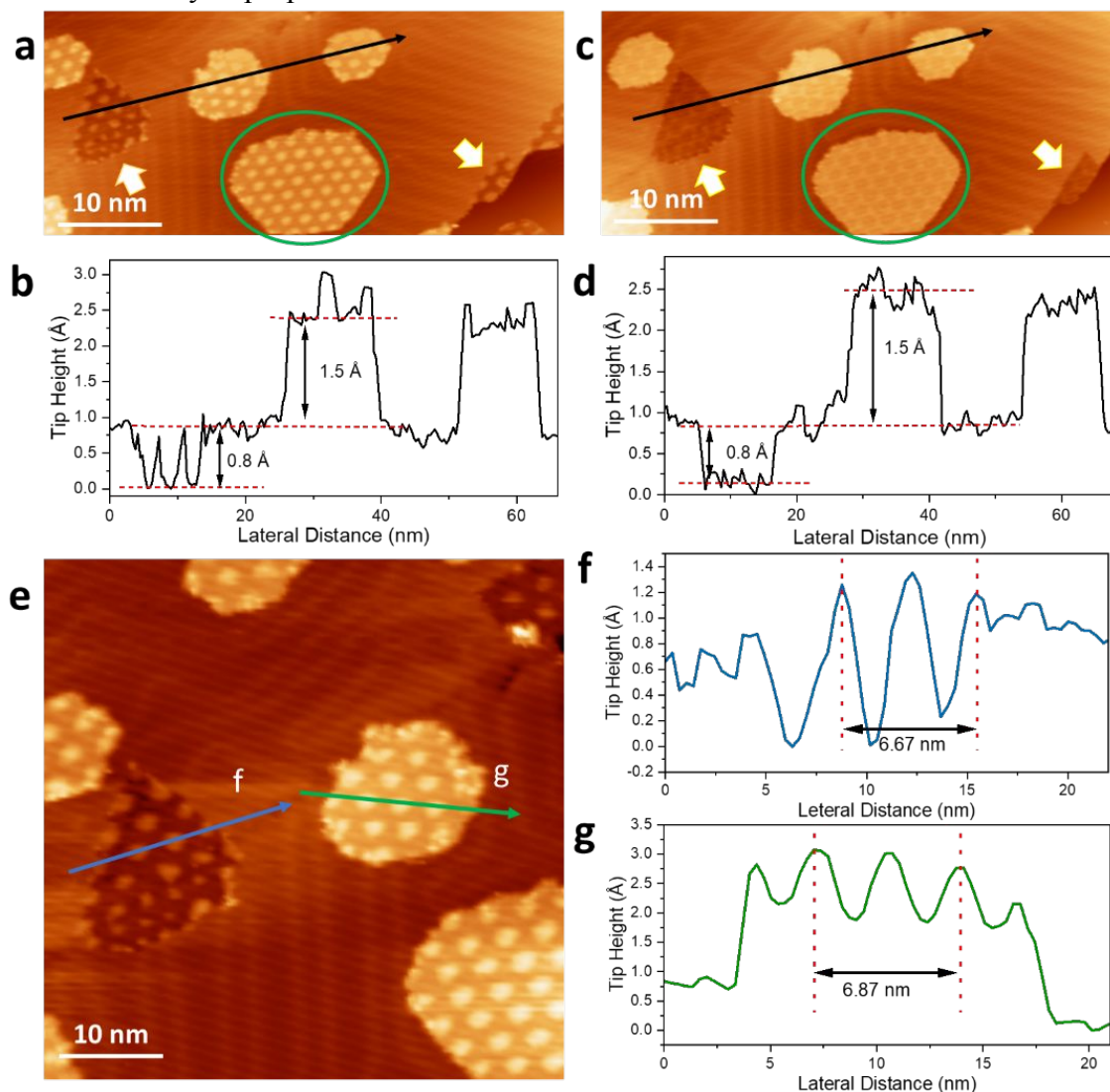


Fig. 3 Bias-dependent STM topography of FeO islands. (a, c) STM images of the same surface obtained under $V_{\text{bias}} = 1.7$ V (a) and -0.8 V (c) and the same tunneling current $I = 0.3$ nA. The green circles highlight the same FeO island with different moiré patterns, and the white arrows point to embedded FeO at the center and edge of the terrace. (b, d) Line profiles along the black lines in (a) and (c), respectively. (e) A close look at embedded and supported FeO islands ($V_{\text{bias}} = 1.7$ V, $I = 0.3$ nA). Height profiles of embedded FeO (f) and supported FeO (g), respectively.

Due to their strong interactions with FeO,²² some transition metals can potentially take up the CUFs at certain FeO edges, thereby selectively exposing other edges for catalytic reactions of interest. Similar research has been done on bi-layer CoO, where the Fe dopant will take up the metal edges of bi-layer CoO and increase the catalysis activity of the sample.⁵⁶ Here, Pd and Pt were used due to their strong interactions with FeO.^{7, 57} As depicted in Fig. 3a, as-deposited Pd atoms distribute randomly on Au(111) surfaces and FeO edges as small clusters. In particular, no preference for Pd adsorption on a certain type of FeO edge was observed at room temperature. In

contrast, upon annealing to 500 K, except for some Pd clusters located in the interiors of FeO islands, the Au(111) supported Pd was exclusively found on three alternate edges of hexagonal FeO islands, leaving the other three adsorbate-free (Fig. 4b-c and S1). A line profile of two Pd islands (Fig. S5a and c) indicates a height at ~ 2.2 Å, which matches the thickness of a single layer of Pd⁵⁸. Based on results from Wendt's group^{50, 51}, FeO islands are slightly reduced in the preparation process. Thereby, O-edges are often disrupted, leading to short and defective edges, while Fe-edges are mostly perfect and longer than O-edges. We observed the same differences between the O- and Fe-edges as shown in Fig. 5, where the blue arrows point to relatively shorter edges with many defects, while the green arrows point to the perfect long edges, which are assigned to O-edges and Fe-edges, respectively. Therefore, the adsorbed edges are identified as Fe-edges, as demonstrated in the caption of Fig. 5. Notably, two different orientations of FeO islands are identified as pointed-top and pointed-bottom configurations (Fig. 4b), which have slightly different atomic structures.^{24, 51} Our results show that Pd selectively grows on the Fe-edges of both pointed-top and pointed-bottom islands, indicating that the selectivity of Pd growth is only related to the type rather than the orientation of the FeO edges. The close affinity of Pd toward Fe-edges is also observed on the embedded FeO islands along Au step edges (right upper part of Fig. 4b) where exposed O-edges, Pd-FeO and Au-FeO interfaces coexist, enabling the comparison of the catalytic behaviors of these interfaces. It is noteworthy that with increasing Pd deposition, all FeO edges including O-edges can be covered (Fig. S3), allowing the catalytic properties of O-edges to be explicitly identified by controlled experiments on FeO with and without exposed O-edges.

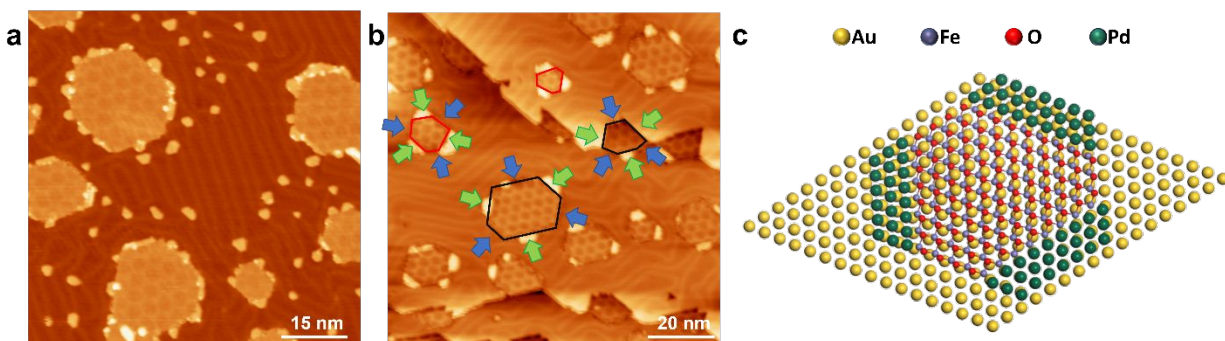


Fig. 4 STM topography of Pd modified FeO/Au(111). (a) As-deposited Pd on FeO/Au(111) ($V_{\text{bias}} = 1.5$ V, $I = 0.3$ nA). (b) Selective growth of Pd on FeO edges following annealing at 550 K ($V_{\text{bias}} = -0.8$ V, $I = 0.3$ nA). The green arrows point to Fe-edges while blue arrows point to O-edges, black and red hexagons indicate pointed-top and pointed-bottom configurations of FeO islands, respectively. (c) Schematic illustration of the atomic structure of Pd-FeO/Au(111).

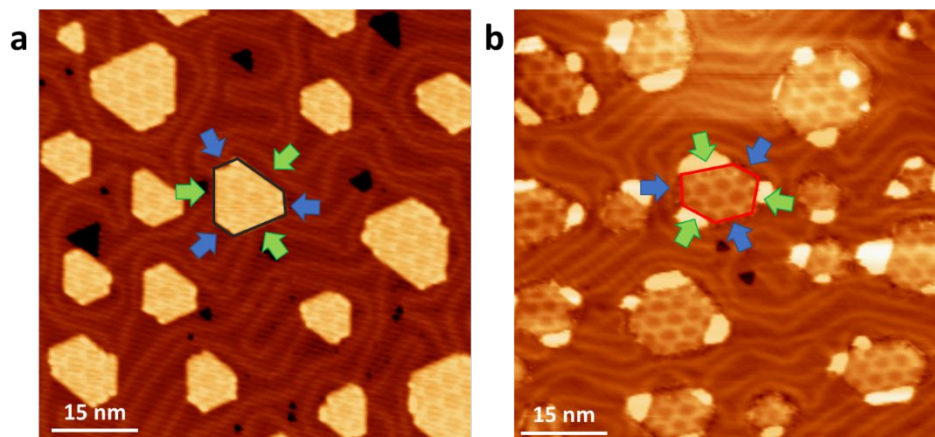


Fig. 5 Edge assignments for (a) FeO/Au(111) ($V_{\text{bias}} = -1.0$ V, $I = 0.3$ nA) and (b) Pd-FeO/Au(111) ($V_{\text{bias}} = -0.8$ V, $I = 0.3$ nA). The blue arrows point to the O-edges while the green arrows point to the Fe-edges. Based on the literature, the short and long edges are O-edges and Fe-edges, respectively. Therefore, the edge assignment is done by first assigning the shortest edge of an island to an O-edge, then identifying the other two alternate O-edges by symmetry, and finally assigning the rest of the edges to Fe edges. The black and red hexagons indicate pointed-top and pointed-bottom configurations of FeO islands.

In addition to Fe-edges, it is desirable to realize the selective exposure of O-edges to enable a comparative study of the two edges. To this end, we investigated the growth of Pt on the FeO/Au(111) surface. Comparing to Pd, Pt has very similar chemical properties, but slightly different metal affinities, which may lead to different selectivity.^{22, 52, 59-61} Similar to Pd, Pt clusters adsorb uniformly on Au(111) surfaces and FeO edges at room temperature (Fig. 6a). However, after annealing to 500 K, single-layer Au(111) supported Pt islands⁶² are found to grow along the short edges of FeO islands that are identified as O-edges (Fig. 6b-c, S2 and S5c). In contrast, all the Fe-edges are exposed. Considering that Pd and Pt have similar affinity to O, the different selectivity between Pd and Pt may be attributed to the relatively weaker interaction of Pt with Fe than O, which results in Pt blocked O-edges.⁵² Consequently, under the same conditions, Pt and Pd have opposite selectivity to the edges of FeO.

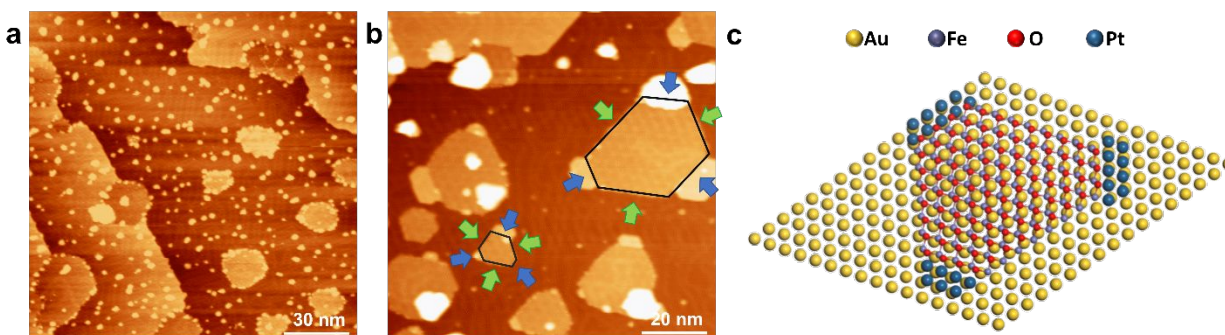


Fig. 6 STM images of Pt modified FeO/Au(111). (a) As-deposited Pt on FeO/Au(111) surfaces ($V_{\text{bias}} = 1.5$ V, $I = 0.2$ nA). (b) Selective growth of Pt on FeO edges following annealing at 550 K ($V_{\text{bias}} = 1.6$ V, $I = 0.2$ nA), the green arrows point to Fe-edges while the blue arrows point to the O-edges. (c) Schematic illustration of the atomic structure of Pt-FeO/Au(111).

It is notable that although the CUFs of FeO islands are buried, due to the high reactivity of Pd and Pt, CO oxidation could occur through catalysis by Pd/Pt⁶³⁻⁶⁵. Under such circumstances, our model can still be used to evaluate the effect of Pd/Pt. As schematically shown in Fig S4, there are four different types of FeO coexisting in the same sample: FeO with all edges exposed, FeO with O or Fe edges blocked, embedded FeO with all edges blocked, and Pd/Pt decorated embedded FeO. By comparing the reactivity of these types of FeO islands, the catalytic activities of pure FeO and Au/Pd/Pt decorated FeO can be evaluated. Meanwhile, as shown in Fig S4d, the selective growth of metals on the edge of embedded FeO results in the coexistence of Au-FeO and Pd/Pt-FeO interfaces, which provides a platform for interrogating the catalytic properties of various metal-FeO interfaces.

Conclusion

In this work, by taking advantage of their different metal affinities, Pd and Pt were selectively grown on the Fe-edges or O-edges of Au(111) supported FeO islands. Our STM studies demonstrated that O-edges and Fe-edges could be exposed separately in a well-controlled manner by the preferential growth of Pd on Fe-edges and Pt on O-edges, respectively. We observed the coexistence of various types of interfaces in one FeO island, which provides a model for comparing the catalytic behaviors at complicated interfaces. With the selectivity growth that we demonstrate here, edge-specific catalytic properties of FeO can be evaluated, thereby shedding light on possible ways to improve catalytic performance.

Conflict of interest

There are no conflicts to declare.

Acknowledgments

N. J. and L. L. gratefully acknowledge financial support from the National Science Foundation (DMR-2211474). M. T. and B. A. S. G. gratefully acknowledge financial support from the National Science Foundation (CHE-2102622). All authors also gratefully acknowledge Prof. Xu Zhang from California State University Northridge for providing simulation support to this work.

Supporting information

STM images of Pd-FeO/Au(111); STM images of Pt-FeO/Au(111); STM images of high Pd coverage Pd-FeO/Au(111); Schematic diagram of interfaces in a Pt/Pd-FeO/Au(111) system; STM images and line profiles of Pd-FeO/Au(111) and Pt-FeO/Au(111)

Reference

1. H.-J. Freund and G. Pacchioni, Oxide ultra-thin films on metals: new materials for the design of supported metal catalysts, *Chem. Soc. Rev.*, 2008, **37**, 2224-2242.
2. W. Weiss and W. Ranke, Surface chemistry and catalysis on well-defined epitaxial iron-oxide layers, *Prog. Surf. Sci.*, 2002, **70**, 1-151.
3. E. D. L. Rienks, N. Nilius, L. Giordano, J. Goniakowski, G. Pacchioni, M. P. Felicissimo, T. Risse, H.-P. Rust and H.-J. Freund, Local zero-bias anomaly in tunneling spectra of a transition-metal oxide thin film, *Phys. Rev. B*, 2007, **75**, 205443.
4. G. H. Vurens, M. Salmeron and G. A. Somorjai, Structure, composition and chemisorption studies of thin ordered iron oxide films on platinum (111), *Surf. Sci.*, 1988, **201**, 129-144.
5. Y. K. Kim, Z. Zhang, G. S. Parkinson, S.-C. Li, B. D. Kay and Z. Dohnálek, Reactivity of FeO(111)/Pt(111) with Alcohols, *J. Phys. Chem. C*, 2009, **113**, 20020-20028.
6. D. Faivre, *Iron oxides: from nature to applications*, John Wiley & Sons, 2016.
7. R. M. Cornell and U. Schwertmann, *The Iron Oxides: Structure, Properties, Reactions, Occurrences and Uses*, Wiley, 2003.
8. Y. J. Kim, C. Westphal, R. X. Ynzunza, Z. Wang, H. C. Galloway, M. Salmeron, M. A. Van Hove and C. S. Fadley, The growth of iron oxide films on Pt(111): a combined XPD, STM, and LEED study, *Surf. Sci.*, 1998, **416**, 68-111.
9. L. R. Merte, J. Knudsen, L. C. Grabow, R. T. Vang, E. Lægsgaard, M. Mavrikakis and F. Besenbacher, Correlating STM contrast and atomic-scale structure by chemical modification: Vacancy dislocation loops on FeO/Pt(111), *Surf. Sci.*, 2009, **603**, L15-L18.
10. L. R. Merte, L. C. Grabow, G. Peng, J. Knudsen, H. Zeuthen, W. Kudernatsch, S. Porsgaard, E. Lægsgaard, M. Mavrikakis and F. Besenbacher, Tip-Dependent Scanning Tunneling Microscopy Imaging of Ultrathin FeO Films on Pt(111), *J. Phys. Chem. C*, 2011, **115**, 2089-2099.
11. H. C. Galloway, J. J. Benítez and M. Salmeron, The structure of monolayer films of FeO on Pt(111), *Surf. Sci.*, 1993, **298**, 127-133.
12. S. Shaikhutdinov, M. Ritter and W. Weiss, Hexagonal heterolayers on a square lattice: A combined STM and LEED study of FeO(111) on Pt(100), *Phys. Rev. B*, 2000, **62**, 7535-7541.
13. H. Zeuthen, W. Kudernatsch, G. Peng, L. R. Merte, L. K. Ono, L. Lammich, Y. Bai, L. C. Grabow, M. Mavrikakis, S. Wendt and F. Besenbacher, Structure of Stoichiometric and Oxygen-Rich Ultrathin FeO(111) Films Grown on Pd(111), *J. Phys. Chem. C*, 2013, **117**, 15155-15163.
14. D. Kuhness, S. Pomp, V. Mankad, G. Barcaro, L. Sementa, A. Fortunelli, F. P. Netzer and S. Surnev, Two-dimensional iron oxide bi- and trilayer structures on Pd(100), *Surf. Sci.*, 2016, **645**, 13-22.
15. J. S. Corneille, J.-W. He and D. W. Goodman, Preparation and characterization of ultra-thin iron oxide films on a Mo(100) surface, *Surf. Sci.*, 1995, **338**, 211-224.
16. J. Karunamuni, R. L. Kurtz and R. L. Stockbauer, Growth of iron oxide on Cu(001) at elevated temperature, *Surf. Sci.*, 1999, **442**, 223-238.
17. C. Pflitsch, R. David, L. K. Verheij and R. Franchy, Preparation of a well ordered iron oxide on Cu(110), *Surf. Sci.*, 2001, **488**, 32-42.
18. I. Palacio, M. Monti, J. F. Marco, K. F. McCarty and J. de la Figuera, Initial stages of FeO growth on Ru(0001), *J. Phys.: Condens. Matter*, 2013, **25**, 484001.
19. Y. Wang, G. Carraro, H. Dawczak-Dębicki, K. Synoradzki, L. Savio and M. Lewandowski, Reversible and irreversible structural changes in FeO/Ru(0 0 0 1) model catalyst subjected to atomic oxygen, *Appl. Surf. Sci.*, 2020, **528**, 146032.
20. X. Deng and C. Matranga, Selective Growth of Fe₂O₃ Nanoparticles and Islands on Au(111), *J. Phys. Chem. C*, 2009, **113**, 11104-11109.
21. N. A. Khan and C. Matranga, Nucleation and growth of Fe and FeO nanoparticles and films on Au(111), *Surf. Sci.*, 2008, **602**, 932-942.

22. Y. Ning, M. Wei, L. Yu, F. Yang, R. Chang, Z. Liu, Q. Fu and X. Bao, Nature of Interface Confinement Effect in Oxide/Metal Catalysts, *J. Phys. Chem. C*, 2015, **119**, 27556-27561.
23. L. Yu, Y. Liu, F. Yang, J. Evans, J. A. Rodriguez and P. Liu, CO Oxidation on Gold-Supported Iron Oxides: New Insights into Strong Oxide–Metal Interactions, *J. Phys. Chem. C*, 2015, **119**, 16614-16622.
24. Y. Li, K. C. Adamsen, L. Lammich, J. V. Lauritsen and S. Wendt, Atomic-Scale View of the Oxidation and Reduction of Supported Ultrathin FeO Islands, *ACS Nano*, 2019, **13**, 11632-11641.
25. S. Yang, J. Gou, P. Cheng, L. Chen and K. Wu, Precise determination of moiré pattern in monolayer FeO(111) films on Au(111) by scanning tunneling microscopy, *Phys. Rev. Mater.*, 2020, **4**.
26. Y. Li, X. Zhao, Y. Cui, F. Yang and X. Bao, Oxidation-induced structural transition of two-dimensional iron oxide on Au(111), *J. Phys. D: Appl. Phys.*, 2021, **54**, 204003.
27. G. J. P. Abreu, R. Paniago and H. D. Pfannes, Growth of ultra-thin FeO(100) films on Ag(100): A combined XPS, LEED and CEMS study, *J. Magn. Magn. Mater.*, 2014, **349**, 235-239.
28. L. R. Merte, M. Shipilin, S. Ataran, S. Blomberg, C. Zhang, A. Mikkelsen, J. Gustafson and E. Lundgren, Growth of Ultrathin Iron Oxide Films on Ag(100), *J. Phys. Chem. C*, 2015, **119**, 2572-2582.
29. M. Shipilin, E. Lundgren, J. Gustafson, C. Zhang, F. Bertram, C. Nicklin, C. J. Heard, H. Grönbeck, F. Zhang, J. Choi, V. Mehar, J. F. Weaver and L. R. Merte, Fe Oxides on Ag Surfaces: Structure and Reactivity, *Top. Catal.*, 2016, **60**, 492-502.
30. M. Lewandowski, T. Pabisiak, N. Michalak, Z. Miłosz, V. Babačić, Y. Wang, M. Hermanowicz, K. Palotás, S. Jurga and A. Kiejna, On the Structure of Ultrathin FeO Films on Ag(111), *Nanomaterials*, 2018, **8**, 828.
31. Z. Zhou, P. Liu, F. Yang and X. Bao, Interface-confined triangular FeO_x nanoclusters on Pt(111), *J. Chem. Phys.*, 2019, **151**, 214704.
32. Y. Jiang, Y. Zhu, D. Zhou, Z. Jiang, N. Si, D. Stacchiola and T. Niu, Reversible oxidation and reduction of gold-supported iron oxide islands at room temperature, *J. Chem. Phys.*, 2020, **152**, 074710.
33. K. Zhang, L. Li, J. Goniakowski, C. Noguera, H.-J. Freund and S. Shaikhutdinov, Size effect in two-dimensional oxide-on-metal catalysts of CO oxidation and its connection to oxygen bonding: An experimental and theoretical approach, *J. Catal.*, 2021, **393**, 100-106.
34. L. Giordano, M. Lewandowski, I. M. N. Groot, Y. N. Sun, J. Goniakowski, C. Noguera, S. Shaikhutdinov, G. Pacchioni and H. J. Freund, Oxygen-Induced Transformations of an FeO(111) Film on Pt(111): A Combined DFT and STM Study, *J. Phys. Chem. C*, 2010, **114**, 21504-21509.
35. Y. Liu, F. Yang, Y. Ning, Q. Liu, Y. Zhang, H. Chen and X. Bao, CO adsorption on a Pt(111) surface partially covered with FeO_x nanostructures, *J. Energy. Chem.*, 2017, **26**, 602-607.
36. R. Meyer, D. Lahav, T. Schalow, M. Laurin, B. Brandt, S. Schauermann, S. Guimond, T. Kluner, H. Kuhlenbeck, J. Libuda, S. Shaikhutdinov and H. J. Freund, CO adsorption and thermal stability of Pd deposited on a thin FeO(111) film, *Surf Sci*, 2005, **586**, 174-182.
37. X. Weng, K. Zhang, Q. Pan, Y. Martynova, S. Shaikhutdinov and H.-J. Freund, Support Effects on CO Oxidation on Metal-supported Ultrathin FeO(1 1 1) Films, *ChemCatChem*, 2017, **9**, 705-712.
38. B. Qiao, A. Wang, X. Yang, L. F. Allard, Z. Jiang, Y. Cui, J. Liu, J. Li and T. Zhang, Single-atom catalysis of CO oxidation using Pt1/FeO_x, *Nat. Chem.*, 2011, **3**, 634-641.
39. X.-K. Gu, R. Ouyang, D. Sun, H.-Y. Su and W.-X. Li, CO Oxidation at the Perimeters of an FeO/Pt(111) Interface and how Water Promotes the Activity: A First-Principles Study, *ChemSusChem*, 2012, **5**, 871-878.
40. M. Lewandowski, I. M. N. Groot, S. Shaikhutdinov and H. J. Freund, Scanning tunneling microscopy evidence for the Mars-van Krevelen type mechanism of low temperature CO oxidation on an FeO(111) film on Pt(111), *Catal. Today*, 2012, **181**, 52-55.

41. Y. N. Sun, L. Giordano, J. Goniakowski, M. Lewandowski, Z. H. Qin, C. Noguera, S. Shaikhutdinov, G. Pacchioni and H. J. Freund, The interplay between structure and CO oxidation catalysis on metal-supported ultrathin oxide films, *Angew. Chem. Int. Ed. Engl.*, 2010, **49**, 4418-4421.
42. T. Yang, T. T. Song, M. Callsen, J. Zhou, J. W. Chai, Y. P. Feng, S. J. Wang and M. Yang, Atomically Thin 2D Transition Metal Oxides: Structural Reconstruction, Interaction with Substrates, and Potential Applications, *Adv. Mater. Interfaces*, 2019, **6**, 1801160.
43. Q. Fu, W. X. Li, Y. Yao, H. Liu, H. Y. Su, D. Ma, X. K. Gu, L. Chen, Z. Wang, H. Zhang, B. Wang and X. Bao, Interface-confined ferrous centers for catalytic oxidation, *Science*, 2010, **328**, 1141-1144.
44. H. Chen, Y. Liu, F. Yang, M. Wei, X. Zhao, Y. Ning, Q. Liu, Y. Zhang, Q. Fu and X. Bao, Active Phase of FeOx/Pt Catalysts in Low-Temperature CO Oxidation and Preferential Oxidation of CO Reaction, *J. Phys. Chem. C*, 2017, **121**, 10398-10405.
45. D. Sun, X.-K. Gu, R. Ouyang, H.-Y. Su, Q. Fu, X. Bao and W.-X. Li, Theoretical Study of the Role of a Metal-Cation Ensemble at the Oxide-Metal Boundary on CO Oxidation, *J. Phys. Chem. C*, 2012, **116**, 7491-7498.
46. K. Zhang, L. Li, S. Shaikhutdinov and H. J. Freund, Carbon Monoxide Oxidation on Metal-Supported Monolayer Oxide Films: Establishing Which Interface is Active, *Angew. Chem. Int. Ed. Engl.*, 2018, **57**, 1261-1265.
47. W. Wang, H. Zhang, W. Wang, A. Zhao, B. Wang and J. G. Hou, Observation of water dissociation on nanometer-sized FeO islands grown on Pt(111), *Chem. Phys. Lett.*, 2010, **500**, 76-81.
48. Y. Yao, Q. Fu, Z. Wang, D. Tan and X. Bao, Growth and Characterization of Two-Dimensional FeO Nanoislands Supported on Pt(111), *J. Phys. Chem. C*, 2010, **114**, 17069-17079.
49. L. Xu, Z. Wu, Y. Zhang, B. Chen, Z. Jiang, Y. Ma and W. Huang, Hydroxyls-Involved Interfacial CO Oxidation Catalyzed by FeOx(111) Monolayer Islands Supported on Pt(111) and the Unique Role of Oxygen Vacancy, *J. Phys. Chem. C*, 2011, **115**, 14290-14299.
50. W. Kudernatsch, G. Peng, H. Zeuthen, Y. Bai, L. R. Merte, L. Lammich, F. Besenbacher, M. Mavrikakis and S. Wendt, Direct Visualization of Catalytically Active Sites at the FeO-Pt(111) Interface, *ACS Nano*, 2015, **9**, 7804-7814.
51. H. Zeuthen, W. Kudernatsch, L. R. Merte, L. K. Ono, L. Lammich, F. Besenbacher and S. Wendt, Unraveling the Edge Structures of Platinum(111)-Supported Ultrathin FeO Islands: The Influence of Oxidation State, *ACS Nano*, 2015, **9**, 573-583.
52. W. T. Geng, A. J. Freeman and G. B. Olson, Influence of alloying additions on grain boundary cohesion of transition metals: First-principles determination and its phenomenological extension, *Phys. Rev. B*, 2001, **63**, 165415.
53. I. Horcas, R. Fernández, J. M. Gómez-Rodríguez, J. Colchero, J. Gómez-Herrero and A. M. Baro, WSXM: A software for scanning probe microscopy and a tool for nanotechnology, *Rev. Sci. Instrum.*, 2007, **78**, 013705.
54. Y. Li, B. Yang, M. Xia, F. Yang and X. Bao, Oxidation-induced segregation of FeO on the Pd-Fe alloy surface, *Appl. Surf. Sci.*, 2020, **525**, 146484.
55. Y. Jiang, S. Bu, D. Zhou, X. Shi, F. Pan, Q. Ji and T. Niu, Two-Dimensional Iron Oxide on Au(111): Growth Mechanism and Interfacial Properties, *J. Phys. Chem. C*, 2021, **125**, 24755-24763.
56. Z. Sun, A. Curto, J. Rodríguez-Fernández, Z. Wang, A. Parikh, J. Fester, M. Dong, A. Vojvodic and J. V. Lauritsen, The Effect of Fe Dopant Location in Co(Fe)OOHx Nanoparticles for the Oxygen Evolution Reaction, *ACS Nano*, 2021, **15**, 18226-18236.
57. S. J. Tauster, S. C. Fung and R. L. Garten, Strong metal-support interactions. Group 8 noble metals supported on titanium dioxide, *J. Am. Chem. Soc.*, 1978, **100**, 170-175.

58. A. W. Stephenson, C. J. Baddeley, M. S. Tikhov and R. M. Lambert, Nucleation and growth of catalytically active Pd islands on Au(111)-22 × studied by scanning tunnelling microscopy, *Surf. Sci.*, 1998, **398**, 172-183.
59. T. B. Reed, *Free energy of formation of binary compounds*, MIT press, 1971.
60. L. Liu, F. Zhou, L. Wang, X. Qi, F. Shi and Y. Deng, Low-temperature CO oxidation over supported Pt, Pd catalysts: Particular role of FeOx support for oxygen supply during reactions, *J. Catal.*, 2010, **274**, 1-10.
61. M. A. van Spronsen, J. W. M. Frenken and I. M. N. Groot, Surface science under reaction conditions: CO oxidation on Pt and Pd model catalysts, *Chem. Soc. Rev.*, 2017, **46**, 4347-4374.
62. J.-H. Zhong, X. Jin, L. Meng, X. Wang, H.-S. Su, Z.-L. Yang, C. T. Williams and B. Ren, Probing the electronic and catalytic properties of a bimetallic surface with 3 nm resolution, *Nature Nanotechnology*, 2017, **12**, 132-136.
63. Y. J. Mergler, A. van Aalst, J. van Delft and B. E. Nieuwenhuys, CO oxidation over promoted Pt catalysts, *Applied Catalysis B: Environmental*, 1996, **10**, 245-261.
64. M. S. Chen, Y. Cai, Z. Yan, K. K. Gath, S. Axnanda and D. W. Goodman, Highly active surfaces for CO oxidation on Rh, Pd, and Pt, *Surf. Sci.*, 2007, **601**, 5326-5331.
65. Z. Duan and G. Henkelman, CO Oxidation on the Pd(111) Surface, *ACS Catalysis*, 2014, **4**, 3435-3443.

